Individual alpha frequency modulates prediction error-driven memory encoding

Sophie Jano[a], Alex Chatburn[a], Zachariah Cross[b], Matthias Schlesewsky[a], Ina Bornkessel-Schlesewsky[a]

[a]Cognitive Neuroscience Laboratory, University of South Australia, St Bernards Road, Magill SA 5072, Australia.
[b]Feinberg School of Medicine, Northwestern University, 420 E Superior St, Chicago, IL 60611, United States.

Corresponding author: Sophie Jano (email: sophie.jano@mymail.unisa.edu.au)

Funding: This research did not receive any specific grant from funding agencies in the public, commercial, or not-for-profit sectors.

Competing interests: The authors have no competing interests to declare.

Abstract

Prediction and memory are strongly intertwined, with predictions relying on memory retrieval, whilst also influencing memory encoding. However, it is unclear how prediction errors during learning, as measured by the N400 event-related potential (ERP), influence explicit memory performance, and how individual neural factors may modulate this relationship. The current study sought to investigate the effect of prediction and individual neural variability on memory processing, whilst exploring the N400 as a prediction error signal in a context extending beyond language. Participants (N = 48, females = 33) completed a study-test paradigm where they first viewed predictable and unpredictable four-item 'ABCD' sequences of outdoor scene images, whilst their brain activity was recorded using electroencephalography (EEG). Subsequently, their memory for the images was tested, and N400 patterns during learning were compared with memory outcomes. Strikingly, greater N400 amplitudes during learning were associated with enhanced memory at test for individuals with low versus high individual alpha frequencies (IAFs). This indicates that IAF may influence stimulus precision weightings and the extent to which prediction errors drive memory encoding. Memory was also strongest for predictable images in the 'B' position, suggesting that when processing longer sequences, the brain may prioritise the data deemed most informative for predictive model updating. Ultimately, the results provide novel insight into the effect of prediction on memory, by highlighting the role of inter-subject variability, whilst shedding light on the accumulation of predictions across sequences.

Keywords: prediction, memory, event-related potentials, EEG

1. Introduction

Modern conceptualisations of memory highlight its importance for predicting the future as opposed to purely remembering the past (Bar, 2007; Exton-McGuinness et al., 2015). According to predictive coding, the brain generates predictions about future inputs from prior experience, which are refined according to prediction errors (mismatches between the prediction and the incoming sensory input; Friston, 2010; Friston & Kiebel, 2009; Hohwy, 2013; Rao & Ballard, 1999). This refinement optimises predictions towards a maximisation of explanatory power, such that the causes of sensory inputs are more accurately inferred and error (or surprise) in the system is reduced (Bastos et al., 2012; Friston, 2010). Predictions allow the brain to cope with complex information whilst reducing free energy in the system (Friston, 2005, 2009, 2010). However, the consequences of prediction for learning and memory are not entirely evident, with the relationship between memory and predictive processing stemming from a reliance of predictions on past experiences (requiring the retrieval of established memory representations; Chow et al., 2016; Rauss & Born, 2017; Schoknecht et al., 2022), and from the effect of prediction on information uptake (concerning memory encoding; Kim et al., 2020; Sherman & Turk-Browne, 2020). Therefore, not only do predictions appear to rely on memory, but predictive processing may have implications for informational accuracy and biases. The present experiment sought to shed light on the effect of prediction on memory performance via an investigation into the neural underpinnings of prediction across sequences.

1.1. Predictions rely on memories of statistical relationships

The notion that predictions rely on memory representations is grounded in the brain's ability to extract environmental regularities – a process known as statistical learning (Turk-Browne in Dodd & Flowers, 2012; Siegelman & Frost, 2015). Regularities are abundant in the natural world, such that similar patterns are encountered across time and space (Turk-Browne in Dodd & Flowers, 2012, p. 118). There is strong evidence that the brain can learn and encode patterns of this nature into memory (i.e., that it can engage in statistical learning); for example, classic visual statistical learning tasks show successful learning of triplets of shapes (Fiser & Aslin, 2002) and syllables (Saffran et al., 1996), presented in a continuous sequence (for similar research in mice, see Gavornik & Bear, 2014). This learning also appears relatively implicit, with participants judging patterns as more familiar than random shapes despite being unaware of an underlying relationship and having low confidence in their decisions (Turk-Browne in Dodd & Flowers, 2012, p. 123). This proficiency for pattern learning has been shown to facilitate predictive processing, with research demonstrating enhanced prediction of upcoming visual orientations following structured versus random sequences (Baker et al., 2014). Additionally, studies employing Serial Reaction Time tasks have revealed faster reaction times for spatial locations that were preceded by predictable versus unpredictable sequences (Nissen & Bullemer, 1987, in Schwarb & Schumacher, 2012). As such, a statistical learning mechanism within memory has been proposed, where statistical relationships are encoded as generalized memory traces to enable the anticipation of future states (Bar, 2007; Turk-Browne in Dodd & Flowers, 2012; Sherman & Turk-Browne, 2020). Statistical learning may thus act as a precursor to the formation of a predictive model (Rauss & Born, 2017), such that regularities are learnt and stored as associative traces in memory, which are subsequently retrieved for future use (Bar, 2007). This highlights the reliance of prediction on memory, with both processes proposed to be functionally similar due to their shared engagement of the hippocampus (Barron et al., 2020). This common hippocampal dependence, coupled with the brain's ability to encode environmental regularities into memory, places statistical learning and

the retrieval of statistical regularities from memory, as likely prerequisites for predictive processing.

1.2. Predictive processing influences memory encoding

The dependence of both memory and prediction on the hippocampus may additionally explain the role of prediction in regulating memory encoding. Prior research has demonstrated poorer memory for stimuli that are predictive of upcoming items, suggesting that the brain may be unable to predict information and encode new memories simultaneously (Sherman et al., 2022; Sherman & Turk-Browne, 2020). According to Sherman & Turk-Browne (2020), prediction may expend hippocampal memory retrieval resources that cannot be concurrently used to encode new traces. In the face of a prediction violation, the hippocampus is proposed to switch to an encoding state to incorporate the sensory information (Mack et al., 2018; Sinclair et al., 2021). This suggests that prediction errors may drive the formation of new memories; a proposal that is supported by behavioural research demonstrating enhanced memory for incongruent stimuli such as reward prediction errors (Jang et al., 2019; Rouhani et al., 2018), surprising images (Greve et al., 2017; Michelon et al., 2003), bizarre sentences (Worthen & Roark, 2002), novel words (Habib et al., 2003), and unpredictable, implausible nouns (however, see Haeuser & Kray, 2022 for a discussion of this effect as being driven by the implausibility of the word, as opposed to the predictability alone). To further support the suggestion that the brain prioritises prediction errors, Furutachi and colleagues (2023) observed amplified sensory representations in the visual cortex of mice for prediction error-eliciting stimuli. As increased brain activity at the time of encoding has been positively correlated with memory outcomes (Kim, 2011), the amplification of error-inducing data may promote stronger memory performance. As such, the prediction error signals resulting from expectation violations may disrupt predictive processing, such that the brain switches to an encoding state to prioritise updating of the incoming information into the predictive model. Naturally, such a mechanism would likely have important consequences for everyday functioning, as novel information may be prioritised during memory encoding.

Although prediction error-eliciting information may be preferentially encoded into memory, other research demonstrates better memory for stimuli eliciting low prediction error (i.e., predictable information; Turan et al., 2023), or for both highly expected and unexpected stimuli, in contrast to moderately expected information (Quent et al., 2022). This has prompted the suggestion that the relationship between predictability and memory follows a U-shaped, nonlinear pattern, such that schema-congruent and schema-incongruent information is prioritised in memory (with schemas proposed to form the basis of predictions; Quent et al., 2022; Van Kesteren et al., 2012). On a similar note, Bein and colleagues (2023) propose that consistency with expectations promotes the integration of that information into existing memory representations. However, prediction errors can promote both integration and memory separation, depending on a number of factors (e.g., the type of prediction error and the strength of the memory reactivation associated with a prediction; Bein et al., 2023). This emphasises the mixed nature of the current literature and the importance of further research into the effect of prediction on memory. If predictive processing regulates information uptake, the predictive model applied and the degree to which the sensory information violates this model may influence what is deemed surprising and what is subsequently encoded into memory. Importantly, whilst most studies assume that incongruent information evokes greater prediction error signals (e.g., Greve et al., 2017; Turan et al., 2023), investigating the neural underpinnings of prediction error is important when determining whether it is in fact the degree of prediction mismatch that drives the observed memory enhancement effects, or whether another factor may account for the observed patterns.

1.3. The N400 event-related potential (ERP) as an index of prediction error

A neural correlate frequently related to prediction error is the N400 event-related potential (ERP), a negative-going component arising approximately 400ms post-stimulus onset (e.g., Bornkessel-Schlesewsky & Schlesewsky, 2019; Fitz & Chang, 2019; Hodapp & Rabovsky, 2021; Kutas & Hillyard, 1980; Rabovsky et al., 2018). The N400 exhibits greater amplitudes following incongruent or unexpected words (e.g., Federmeier & Kutas, 1999; Kutas & Hillyard, 1980, 1984), with the amplitude increasing in a graded fashion as word predictability decreases (DeLong et al., 2005). Consequently, recent perspectives posit that the component reflects the degree of mismatch between a prediction and the sensory input (i.e., a prediction error; Bornkessel-Schlesewsky & Schlesewsky, 2019; Hodapp & Rabovsky, 2021), with this perspective explaining prediction in contexts that extend beyond language (e.g., see Urgen et al., 2018 for a discussion of the N400 in relation to prediction violations and the uncanny valley effect). However, despite the component's applicability to non-linguistic contexts, most research relating the N400 to memory outcomes pertains to language, revealing enhanced implicit memory (as evidenced by faster reaction times) for words that evoked greater N400 amplitudes (Hodapp & Rabovsky, 2021). Meyer and colleagues (2007) also observed that N400 amplitudes to words during learning were correlated with ERP old/new effects reflecting familiarity at test, suggesting that the N400 may support familiarity-based recognition. Other research on repetition suppression provides indirect evidence supporting the role of prediction errors in memory encoding, demonstrating N400 amplitude decreases following repeated exposure to incongruent sentence endings (Besson et al., 1992). This decrease in N400 activity has been interpreted to reflect adaptation of the predictive model to initially unexpected stimuli (Hodapp & Rabovsky, 2021); for similar research on the mismatch negativity (MMN) ERP, see (Garrido et al., 2009). However, repetition suppression effects for incongruent information may not always translate to better memory recall, with Besson and colleagues' (1992) study demonstrating stronger effects of repetition suppression on memory for congruent versus incongruent stimuli. This highlights the importance of further research to test the assumption that prediction errors, as reflected by the N400 component, drive behavioural memory enhancement effects.

If memory encoding is influenced by the degree of prediction error, it may also be susceptible to individual differences in predictive processing. The N400 response has been shown to differ between individuals according to intrinsic neural factors, namely the aperiodic slope of the 1/f distribution and individual alpha frequency (IAF), the peak frequency within the alpha rhythm (Bornkessel-Schlesewsky et al., 2022; Dave et al., 2018; Jano et al., 2023). This suggests that the strength of prediction error signals may differ between subjects to influence memory performance. However, to our knowledge, N400 patterns during learning have not been related to explicit memory outcomes in non-linguistic settings, and with a consideration of intrinsic neural differences. Further, few studies have investigated the accumulation of predictions and their effect on memory across longer sequences of information, with most studies focussing on pairs or triplet relationships (Long et al., 2016; Otsuka & Saiki, 2016; Rouhani et al., 2020; Sherman et al., 2022; Sherman & Turk-Browne, 2020; Turan et al., 2023). However, the temporal accuracy of ERPs may provide a means to track predictions in real-time and across longer associations, to understand how predictions adapt according to information accrual. Therefore, an investigation into the relationship between the N400 and memory across sequences may have important implications for learning in naturalistic settings, where information is received in a continuous stream (Parr et al., 2022). Such an investigation may aid in understanding the consequences of prediction for learning more generally, whilst providing insight into prediction as a probabilistic and adaptive process.

The present study aimed to determine the effect of prediction and individual neural factors on memory via an analysis of the N400 ERP component. Participants first engaged in a learning task where they were exposed to predictable and unpredictable sequences of outdoor scene images, after which their recognition of the images was tested. As prior research suggests that memory is impaired for prediction-related stimuli (Sherman & Turk-Browne, 2020), it was hypothesised that memory performance would be better for images in the unpredictable sequences, in contrast to images in the predictable sequences. Based on prior research highlighting the role of the N400 as a prediction error signal that drives model adaptation (e.g., Rabovsky et al., 2018 in Hodapp & Rabovsky, 2021), it was also hypothesized that N400 amplitude would be positively related to memory recognition, such that greater N400 amplitudes during learning would lead to enhanced memory performance.

2. Materials and methods

2.1. Participants

Fifty individuals took part in the experiment; a sample size based on similar research (Sherman & Turk-Browne, 2020) that aimed to increase statistical power whilst accounting for participant drop-out rates or data corruption. Two participants were removed from the sample, one due to technical difficulties and the other due to misinterpretation of the task instructions. Consequently, the final sample size was 48 (mean age = 27 years old), consisting of 15 males and 33 females. All participants were right-handed adults between the ages of 18 and 40, with normal to corrected-to-normal vision. Participants were not taking regular medication that could impact the EEG and did not have any diagnosed psychiatric conditions (e.g., depression), diagnosed intellectual impairments, or a diagnosis of dyslexia. They also reported no recreational drug use in the past 6 months. Due to the within-groups nature of the study design, all participants were exposed to all experimental conditions (predictable and unpredictable sequences).

2.2. Stimuli and task

2.2.1. Outdoor scene task

LEARNING PHASE: Stimuli during the learning phase of the outdoor scene task consisted of 102 sequences containing four outdoor scene images each (408 images total). Images were adapted from materials obtained from Sherman & Turk-Browne (2020), and belonged to one of twelve categories (beaches, bridges, deserts, forests, fields, lighthouses, mountains, parks, waterfalls, canyons, lakes, and reefs). In contrast to Sherman and Turk-Browne's (2020) experiment, we included the 'reefs' category to replace the category 'marshes,' as many of the images within the 'marshes' category were either of a low resolution or were highly similar to each other, and we believed that they may have been too difficult to distinguish from one another. Images belonging to the 'reefs' category were taken from Google image searches and were identical in size to the images from the other categories (800 x 600 pixels). Images were presented in the centre of the screen using the *Opensesame* program (Mathôt et al., 2012).

Of the 102 sequences in the learning phase, 68 were predictable, as they contained the same image categories in the same A→B→C→D order (either PARK → BRIDGE → LIGHTHOUSE → WATERFALL or DESERT → BEACH → FOREST → MOUNTAIN). Although the categories and their order remained stable within the predictable sequences, the

specific image belonging to that category always differed, such that no one image was repeated during learning. This is in line with Sherman and Turk-Browne's (2020) study, which probed item-specific memory whilst retaining predictable relationships in the form of categorical associations. The remaining 34 sequences always consisted of images from the categories CANYONS, REEFS, FIELDS, and LAKES. Images in these sequences were presented in random order, rendering them unpredictable (hence they were labelled 'Z' images). The initial assignment of categories to the two conditions (predictable ABCD sequences and unpredictable Z sequences) was random but did not differ between participants. Further, the order in which each sequence appeared was randomised across participants, although the specific images in each sequence remained consistent between individuals. As the images belonging to 6 of the 12 overall image categories contained a man-made object, it was ensured that this distribution was balanced between the two sequence conditions, such that the predictable (ABCD) sequences contained four (out of eight total) categories with man-made objects, and the unpredictable (Z) sequences (of which there were half as many as the predictable sequences) contained two (out of four) categories with man-made objects.

RECOGNITION PHASE: During the recognition phase, stimuli consisted of the 408 'old' images shown during the learning phase, belonging to both the predictable (ABCD) and unpredictable (Z) sequences. Additionally, 72 'new' lure images that participants were not previously exposed to were included; 48 belonging to the predictable (ABCD) categories, and 24 belonging to the unpredictable (Z) categories. The differing number of lures between the two sequence conditions was proportional to the distribution of sequence types during learning, such that there were double the number of predictable images as compared to unpredictable images (note that this was considered when calculating memory performance). To maintain consistency regarding the distributions of the various image categories, six lures belonged to each of the 12 outdoor scene categories, resulting in 12 lure images per A, B, C, D position for the predictable ABCD sequences. For example, as A images belonged to the 'park' and 'desert' categories, six lures were images of parks, and six were images of deserts. As the Z condition consisted of four image categories (CANYONS, REEFS, FIELDS, and LAKES), six lures from each category were presented. The number of lures per category is adapted from Sherman & Turk-Browne (2020), who presented participants with predictable A → B pairings and included four lures per predictable (AB) category in their recognition phase. As our design was extended to include longer image sequences and unpredictable sequences, we chose six lures per category to account for this increase. All images during the recognition phase were presented sequentially and in a random order across participants. A schematic of the outdoor scene task is presented in *Figure 1*.

Figure 1. Schematic of the outdoor scene task
(a) *The learning phase of the outdoor scene task, where participants were presented with predictable and unpredictable four-item sequences of outdoor scene images. Each image was presented sequentially and was separated by a fixation dot. The below example is of a predictable ABCD sequence (A: desert, B: beach, C: forest, D: mountain).* ***(b)*** *The recognition test phase of the outdoor scene task, where participants were presented with old images from the original learning phase, and new lure images, to which they made an 'old' or 'new' judgement.*

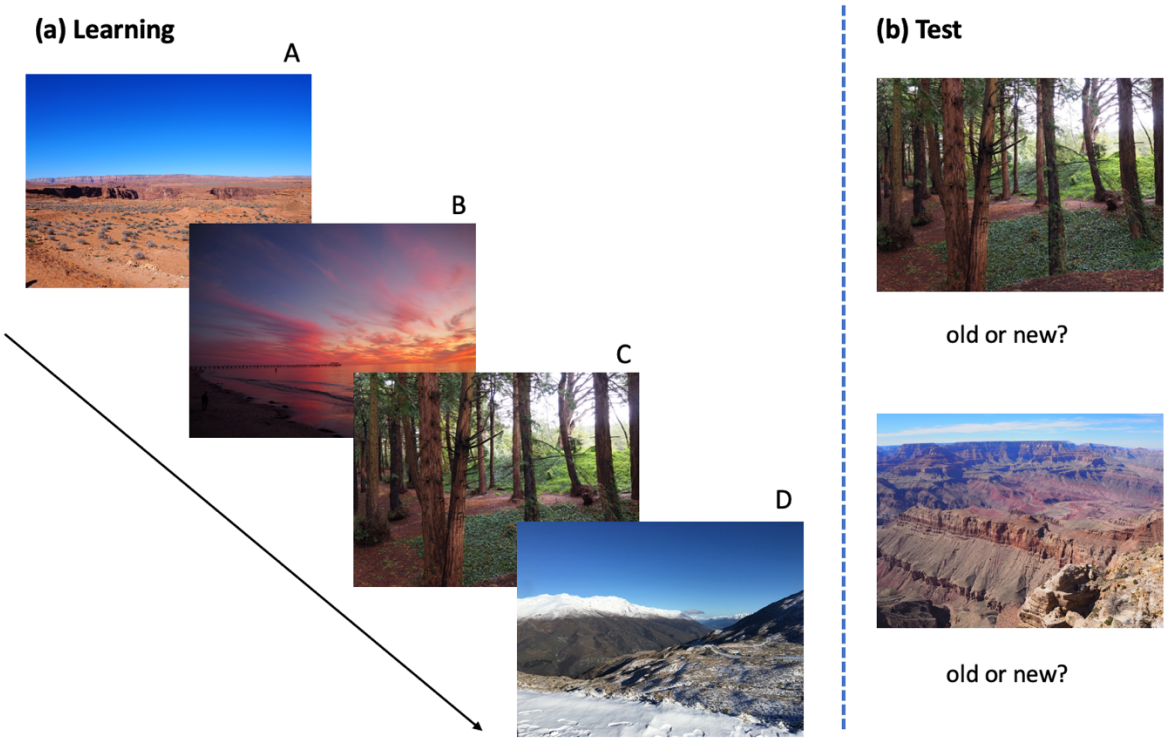

2.3. EEG measures
Electroencephalography (EEG) was recorded throughout the experimental tasks using a 32-channel Brainvision ActiCHamp system (Brain Products GmbH, Gilching, Germany). For the reference electrode, the T7 electrode in the Afz position was used. However, one participant had a faulty T7 electrode, and so the FT9 electrode was used as the reference instead. The ground electrode was placed in the Fpz position and dropdown electrodes from the Fp1 and Fp2 positions were used as the bipolar electrooculogram (EOG) channels, placed above and below the left eye. The data were sampled at a frequency of 500Hz (DC coupled), and the impedances of the channels were maintained below 10kΩ.

2.4. Experimental design and procedure
Ethical approval for the study was first sought from the University of South Australia Human Research Ethics committee. Eligible participants provided written informed consent to participate in the research, after which their EEG was set up by an experienced technician. They were seated at a computer in a quiet testing room, with their eyes closed for two minutes, and then with their eyes open for two minutes, to obtain recordings of their resting state brain activity for the calculation of IAF and aperiodic activity. Following this, participants either engaged in the main outdoor scene task, or completed short control tasks. The order in which

participants completed the main task and the control tasks was counterbalanced between participants to control for fatigue effects.

The procedure for the outdoor scene task is loosely based on Sherman & Turk-Browne (2020)'s protocol. For the learning phase of the outdoor scene task, participants viewed the four-item sequences whilst their EEG was recorded. They were not informed of the underlying patterns amongst the images but were simply told that each sequence would consist of four images, presented one after the other, to which they must pay attention. Each image was presented for 1000ms, followed by a fixation dot in the centre of the screen that was present for 500ms. The between-sequence intervals were 2000ms in duration, to create noticeable boundaries between sequences. As a secondary cover task, throughout the learning phase, a prompt would appear on the screen telling participants to press 'Enter,' as quickly as possible. This would occur at seven random between-sequence intervals during the experiment and would time-out only once the enter key had been pressed. Participants were informed that this was a secondary task to ensure that they were paying attention. The total duration of the learning phase was approximately 15 minutes.

After the learning phase, participants performed a digit span task to minimize recency effects. The task was presented via the OpenSesame program (Mathôt et al., 2012) and took approximately 15 minutes to complete. Following this, participants engaged in a surprise recognition test, where they were presented with old images and new lure images in a random order whilst their brain activity was recorded. For each image, participants were required to state whether the image was 'old' (they saw it in the original learning phase), or 'new' (they did not remember seeing it during the learning phase), using the 'z' and 'm' keys, respectively. Participants responded to the image whilst it was on the screen, with a keypress triggering a switch to a fixation dot with a duration of 500ms. Image presentations timed out after 6 seconds if no response was provided. The duration of the recognition phase was approximately 15 minutes.

The control tasks were completed either before or after the outdoor scene task, with this order counterbalanced between participants to combat fatigue effects. The tasks consisted of a visual statistical learning (VSL) task (Siegelman et al., 2017) that took approximately 20 minutes to complete, and other short tasks. As the control tasks are not the focus of the current investigation, they will not be discussed further. Following completion of the experiment, the EEG cap was removed, and participants were provided with a $50 payment as compensation for their time. The total testing time for the experiment was approximately 2 hours.

3. Data analysis

3.1. d-prime (d') calculation

To quantify participants' recognition accuracy, d-prime (d'; McNicol, 2005) was calculated based on performance during the recognition testing phase of the outdoor scene task. Performance was grouped according to participants' old/new responses, where the number of hits (old images correctly identified as 'old') and false alarms (new images incorrectly judged as 'old') were calculated per image position/condition (predictable A, B, C, D, and unpredictable Z), across participants. Following this, d' scores for each image type (predictable 'A', 'B', 'C', 'D' and unpredictable 'Z' images) were computed using the *psycho* package (Makowski, 2018) in R version 4.3.1, which subtracts the z-score of the false alarm rate from the z-score of the hit rate (McNicol, 2005). Six subjects with false alarm rates equal to zero were identified, and as such, the d' function was run with adjust = 'TRUE' to adjust for extreme

scores in line with Hautus (1995). Note that it was not possible to obtain d' scores for each image position for images in the unpredictable 'Z' condition. This is because lure images were based on categories, but the categories' positions in the unpredictable sequences differed each time (e.g., for one sequence, an image of a canyon might be in the 'A' position, but for the next sequence, a canyon image might be in the 'C' position). As such, d' for unpredictable 'Z' images was calculated across all positions.

Unforeseen technical difficulties were experienced by five participants during the learning phase of the outdoor scene task, such that the task crashed at variable positions. For one participant, the task crashed towards the beginning (after the 32nd sequence), and they completed the learning phase again. The trials that they had seen twice were removed from their behavioural recognition results in case repeated exposure led to enhanced memory performance for those items. For the remaining four participants, the trials that they had not seen during learning were removed from their behavioural results. We adjusted the d' calculations for all of these participants based on the number of lure and target images that were seen. However, one participant appeared to have made an abnormally large number of 'new' judgements, especially to 'old' images that were seen during learning. As this may have reflected a bias in performance (potentially resulting from the participant's belief that they had not seen many of the images), this participant was removed from subsequent analyses.

3.2. EEG data processing

To maintain EEG files in line with recommended standards, the EEG data from the learning phase were first transformed into the Brain Imaging Data Structure (BIDS; Appelhoff et al., 2019) using the *MNE-BIDS* package in MNE-python version 3.8.8 (Gramfort et al., 2013). Subsequent pre-processing occurred using MNE-python, where the data were re-referenced to the mastoid channels (TP9 and TP10). Power spectral density (PSD) plots were then generated, and the data were visually inspected for bad channels, which were marked. Electrooculogram (EOG) channels were set as Fp1 and Fp2 before an independent component analysis (ICA) was fit to a 1Hz high pass filtered copy of the data. The ICA was then applied to the raw data to identify and remove ocular noise, after which bad channels were interpolated using spherical splines. Next, the data was filtered with a bandpass filter ranging from 0.1 to 30Hz.

Following processing, the data were epoched around events of interest, between -0.3ms preceding the images to 1 second post-image (1.3 seconds total duration). Epochs were also generated around the 'A' images in the sequences (0 to 6 seconds duration) to facilitate grand average plotting of the whole sequence. The *Autoreject* function (Jas et al., 2016) was then applied to interpolate and/or remove bad epochs, resulting in an average of 246.9 epochs for predictable images and 123.2 epochs for unpredictable images across participants.

3.3. ERP generation

Event-related potentials (ERPs) were computed using *MNE-Python* (Gramfort et al., 2013) over an N400 window that ranged from 300ms to 500ms post-image onset. As previous research suggests that the N400 in pictorial paradigms exhibits a frontal topography (Kutas & Federmeier, 2011; Urgen et al., 2018), we examined the N400 over frontal channels (Fz, F3, F7, FT9, FC5, FC1, FT10, FC6, FC2, F4, F8). The mean N400 amplitude within the window of interest, per channel, trial and participant was calculated.

ERP grand average plots revealed differences at a later time window that resembled the late positive complex (LPC) ERP. As an additional exploratory analysis, we computed the LPC over a 600ms to 1000ms window post-image onset. Prior research generally examines the LPC

over an approximate 500ms to 800ms window post stimulus onset (Stróżak et al., 2016; Yang et al., 2019), although it has been measured within a 500ms to 1000ms window before (Brezis et al., 2017). We extended the typical window to capture the prominent differences in the component (as identified via visual inspection), whilst avoiding overlap with the subsequent inter-stimulus interval. The LPC was computed over centro-parietal channels (Pz, P3, P4, P7, P8, CP1, CP2, CP5, CP6, C3, C4, Cz), in line with prior research (Finnigan et al., 2002).

Rather than performing a traditional baseline correction, ERP activity was additionally computed over a pre-stimulus window ranging from -300 to 0ms prior to image presentation. Mean pre-stimulus ERP amplitudes were calculated for each channel and trial, and were used as a 'baseline' window, that was included as a covariate in statistical models. This approach is described by Alday (2019) and is proposed to enhance statistical power in contrast to traditional baseline correction methods. To generate ERP grand average plots, the data were resampled to 125Hz, and frequency and amplitude data at each time point within a 6 second window was computed. Grand averages were plotted across the whole sequence using the *ggplot2* package in R version 4.3.1 (Wickham, 2016).

3.4. Individual metrics

To obtain measures of individual alpha frequency (IAF) and the 1/f aperiodic slope, eyes closed data from resting state recordings was used. The data were resampled to 250Hz, re-referenced to TP9 and TP10, and filtered with a bandpass filter from 0.1 to 30Hz. IAF was calculated using the *Philistine* package in *MNE-Python* (Alday, 2019), over electrodes P3, P4, Pz, O1, O2 and Oz, with the lower bound of the alpha frequency set at 7Hz, and an upper limit of 13Hz. This method is based on Corcoran et al. (2018) and calculates both the peak alpha frequency (PAF; the most prominent peak in the alpha spectrum) and the centre of gravity (CoG; the weighted mean of power across the alpha frequency band; Corcoran et al., 2018).

To obtain estimates of the aperiodic 1/f slope, the power spectral density was first calculated across the raw data, for channels P3, P4, Pz, Oz, O1 and O2, to maintain consistency with the IAF metrics. The *Fitting Oscillations and One-Over f (FOOOF)* package (version 1.0.0; Donoghue et al, 2020) was then used to parameterize the power spectrum, which occurred across a 1 to 30Hz frequency range. The *FOOOF* model settings included a fixed aperiodic mode with a peak width limit of two to eight, a peak threshold of two, a minimum peak height of zero, and a maximum number of four peaks. Subsequently, the data were averaged across the three channels, resulting in a single 1/f aperiodic slope measure per participant.

3.5. Statistical analysis

Linear mixed-effects models (LMMs) were computed with the *lme4* package in R version 4.3.1 (Bates et al., 2014) to examine effects of interest, as such models allow for the specification of both fixed and random factors (See *Table 1* for statistical model structures). Whilst random intercepts were included in all models, the inclusion of by-subject and/or by-item random slopes led to convergence issues for some. As such, random slopes were omitted in some cases, as this may reflect overfitting (for a discussion of model overparameterization, see Bates et al., 2018). To calculate *p*-values, type II Wald tests from the *car* package were used (Fox & Weisberg, 2019), which were computed according to an alpha level of 0.05. The categorical variables of condition and position were sum contrast coded using the *contr.sum* function from the *car* package (Fox & Weisberg, 2019), and continuous predictors were scaled and centred. Model effects were visualised with 83% confidence intervals using *ggplot2* (Wickham, 2016). In some cases, IAF and the 1/f slope were included in the same model as separate interaction terms to reduce the number of models. Also note that for statistical models including IAF, CoG

is specifically used as it may be more sensitive when a dominant alpha peak is absent (e.g., in cases where a split peak is observed; Corcoran et al., 2018). Finally, as IAF could not be estimated for two participants, models with IAF were computed with a sample size of 46, whilst models that did not include the factor of IAF included the full sample size of 48 participants.

Table 1.
Linear mixed-effects model structures including outcome variables, fixed effects, covariates, and random intercepts.

Behavioural models

Model	Outcome	Fixed effects	Separate interaction terms	Random intercepts	Random slopes
1	d'	Condition (predictable/ unpredictable)	1/f slope IAF	+ Subject	
2	d'	Image type (predictable A/B/C/D, unpredictable Z)	1/f slope IAF	+ Subject	

ERP models

Model	Outcome	Covariates	Fixed effects	Random intercepts	Random slopes
3	N400 amplitude	Pre-stimulus ERP amplitude	Condition (predictable/ unpredictable) Position (A/B/C/D)	+ Subject + Item	By-subject according to condition

Combined ERP and behavioural models

Model	Outcome	Covariates	Fixed effects	Random intercepts	Random slopes
4	d'	Pre-stimulus ERP amplitude	Condition (predictable/ unpredictable) Position (A/B/C/D) N400 amplitude IAF	+ Subject	By-subject according to condition
5	d'	Pre-stimulus ERP amplitude	Condition (predictable/ unpredictable) Position (A/B/C/D) N400 amplitude 1/f slope	+ Subject	By-subject according to condition

4. Results

Statistical model outputs are presented in the appendix, whilst the data and analysis scripts necessary for replication of the results are freely available at the following repository: https://osf.io/qvjer/.

4.1. Descriptive statistics

The mean reaction time in response to the 'enter' prompt during the cover task of the SRT learning phase was 0.770 seconds (*SD* = 0.395 seconds), suggesting that participants were paying attention to the task. Mean and standard deviation d' scores from the learning phase of the SRT are presented in *Table 2.*

Table 2. Behavioural performance

Mean d' scores per image condition and position, with standard deviations in brackets. Note that d' was computed across all images in the unpredictable 'Z' sequences, regardless of their position, as category lures could not be made specific for each position.

Condition	***Predictable***				***Unpredictable***
Position	**A images**	**B images**	**C images**	**D images**	**Z images**
Mean (*sd*)	0.50 (0.44)	0.69 (0.45)	0.22 (0.37)	0.23 (0.41)	0.31 (0.31)

4.2. Linear mixed-effects models

4.2.1. Behavioural results

To investigate the hypothesis that predictable images would be remembered more poorly than unpredictable images, Model 1 was fitted to the data including the variables of image condition (predictable/unpredictable), IAF and 1/f slope. The model did not detect a significant main effect of condition on d' ($\chi2(1) = 1.98$, $p = 0.160$; See *Figure 2a*). The interaction between IAF and condition was also nonsignificant ($\chi2(1) = 0.68$, $p = 0.41$), in addition to the interaction between condition and 1/f slope ($\chi2(1) = 1.32$, $p = 0.251$).

To investigate the effect of both image condition and image position, the *image type* variable was used for the behavioural analyses, as the levels of this variable were divided into predictable 'A', 'B', 'C' and 'D' images, and unpredictable 'Z' images. To investigate the effect of image type, IAF and the 1/f slope on d' scores, Model 2 was computed. A significant main effect of image type on d' was detected ($\chi2(4) = 50.97$, $p <.001$), such that d' scores were greatest for predictable B images (See *Figure 2b*).

Figure 2. Behavioural data
(a) *d' score predicted by image condition (predictable versus unpredictable).* ***(b)*** *d' score predicted by image type (predictable A, B, C, D, and unpredictable Z images). Faded dots in both plots indicate raw data points, and filled dots reflect predicted model values.*

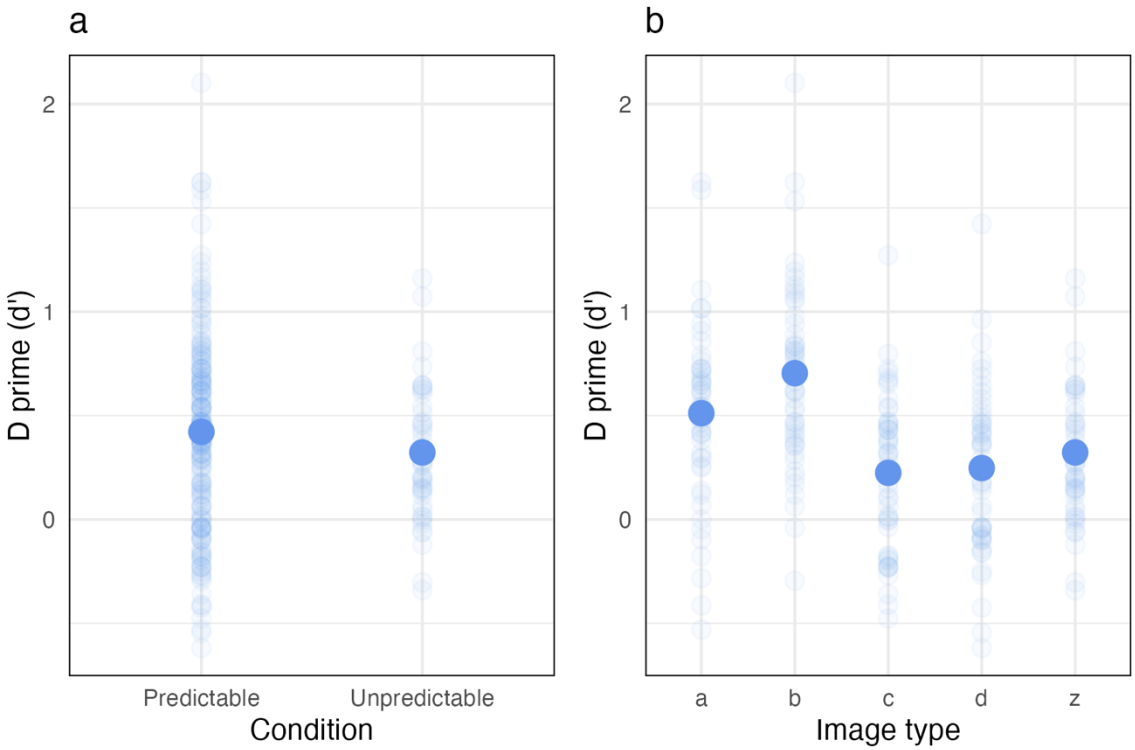

4.2.2. N400 results

Grand average ERP plots of the N400 are presented in *Figure* 3. Visual inspection reveals greater N400 amplitudes for predictable 'A' images, with this pattern reversing as the sequence progresses (showing the opposite pattern at the 'D' image position). Model 3 was fitted to examine the effects of image condition and position on the amplitude of the N400 component. Note that as ERPs were computed at the single trial level (versus subject level for d' scores), the variables 'condition' and 'position' contained differing information and could thus be included in the same model, in contrast to the behavioural models, where *image type* is used. Initially, the model failed to converge with the inclusion of random intercepts of subject, channel, and item, and with random slopes. To simplify the model structures, N400 amplitude was averaged over channels according to regions of interest, and the random intercept of channel was removed. The interaction effect between image condition (predictable/unpredictable) and position (A, B, C, D) was significant ($\chi2(3) = 8.09$, $p < .05$), such that N400 amplitudes were greatest for images in the 'B' position, particularly those in the unpredictable versus predictable sequences (see *Figure 4a*).

Figure 3. N400 grand average ERPs

Grand average plots depicting N400 effects according to image condition (predictable versus unpredictable), across channels Fz, F3 and F4 (for visualisation purposes). Grey shading depicts the N400 window, black dotted lines represent the onset of each image, and grey dotted lines mark the end of image presentation. Blue lines reflect N400 activity in the predictable condition, whilst pink dotted lines represent the unpredictable condition. Blue and pink shading depicts the standard errors for each condition.

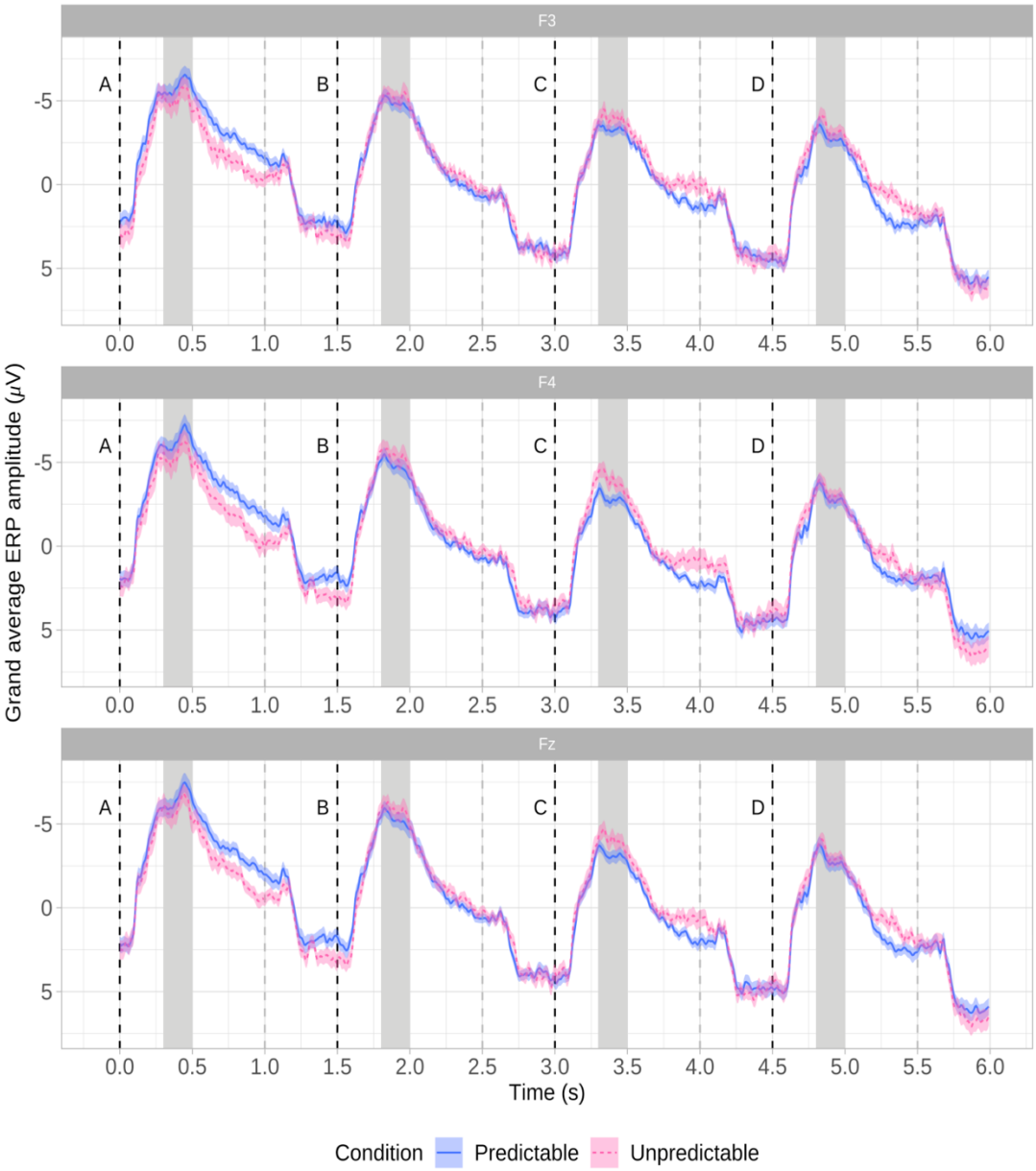

4.2.3. Combined N400 and behavioural results

It was predicted that images that evoked greater N400 amplitudes during learning would be better remembered. To investigate this hypothesis, we ran a combined LMM (Model 4) predicting d' from image condition (predictable/unpredictable), position (A, B, C, D), N400 amplitude, and IAF. Importantly, as d' is an aggregated variable, this analysis could not be completed at the single trial level. Instead, N400 amplitude was averaged such that a mean N400 amplitude score per image condition, position, and subject, was computed. A significant interaction between N400 amplitude and IAF was revealed ($\chi 2(1) = 7.59$, $p < .01$),

such that for low IAF individuals, d' scores increased as N400 amplitudes during learning increased, whilst this pattern was not observed for those with a high IAF (See *Figure 4b*). Model 5 was fitted to investigate the effect of condition (predictable/unpredictable), position (A, B, C, D), N400 amplitude and the 1/f slope on d'. The interaction between the four variables was nonsignificant ($\chi2(3) = 1.38$, $p = .710$). As such, IAF interacted with N400 amplitude to influence d' scores, but the 1/f slope did not.

Figure 4. N400 effects
(a). *The modelled effect of image condition (predictable versus unpredictable) and image position (A, B, C, D) on N400 amplitude. Blue dots represent predictable sequences, whilst pink dots represent unpredictable sequences. Error bars reflect 83% confidence intervals.* ***(b).*** *Linear mixed model results depicting the interaction between N400 amplitude and IAF on d'. Green lines represent low IAFs, whilst blue dotted lines depict high IAFs, with this dichotomisation calculated according to the first and third quartiles for visualisation purposes only. Green and blue shading depicts the 83% confidence intervals.*

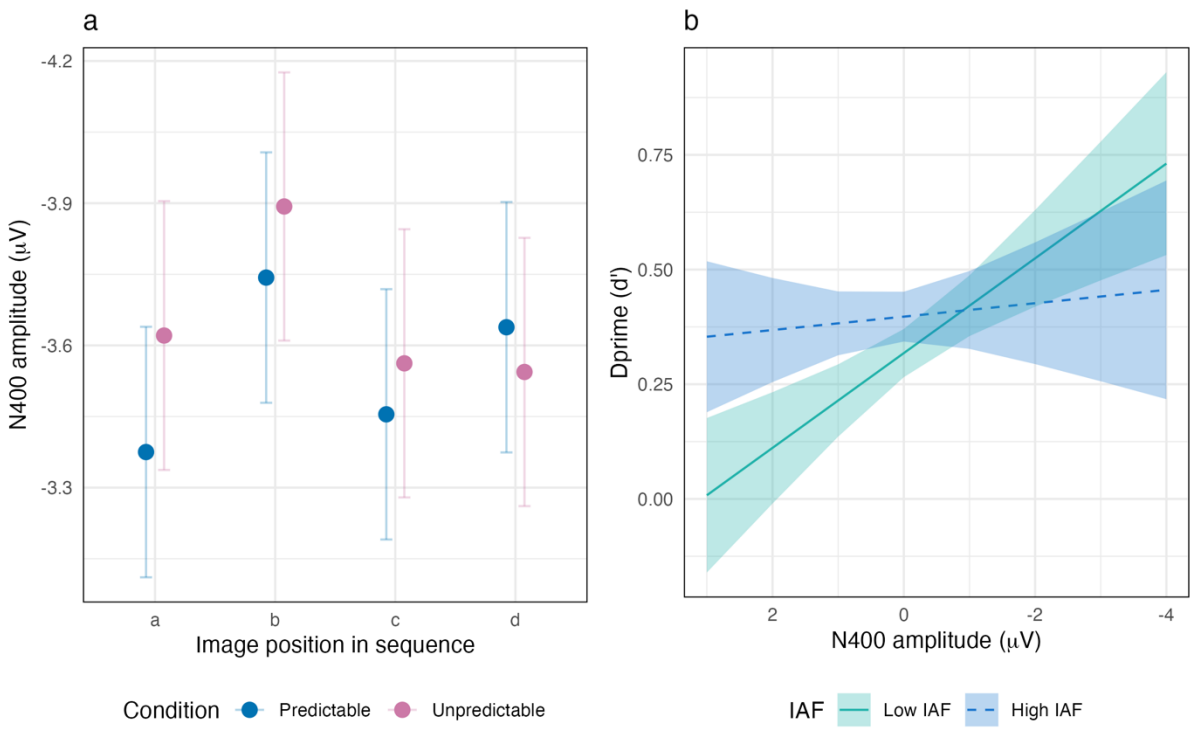

4.3. Exploratory LPC models

As visual inspection of our grand average plots revealed ERP differences in a later window (See *Figure 5*), we also ran exploratory analyses investigating a component resembling the LPC ERP. Exploratory LPC LMM structures are presented in *Table 3*.

To investigate whether the amplitude of the LPC was affected by image condition and position, Model 6 was fitted. Despite averaging over channels of interest to reduce model complexity, the model failed to converge with random slopes, which were consequently omitted. The model revealed a significant interaction effect of condition and position on LPC amplitude ($\chi2(3) = 24.63$, $p < .001$), such that LPC amplitudes were smallest for predictable versus unpredictable images in the A and C positions (See *Figure 6*). Model 7 was fitted to predict d' from LPC amplitude, condition, and position. Similarly to the N400 models, as d' is an aggregate measure, LPC amplitudes were averaged to obtain a mean value per subject, condition and

position. The model did not detect a significant effect of condition, position and LPC amplitude on d' ($\chi2(1) = 3.77$, $p = .287$).

Table 3.
Linear mixed-effects model structures for exploratory LPC analyses, including outcome variables, fixed effects, covariates, and random intercepts.

Model	Outcome	Covariates	Fixed effects	Random intercepts	Random slopes
6	LPC amplitude	Pre-stimulus ERP amplitude	Condition (predictable/ unpredictable) Position (A/B/C/D)	+ Subject + Item	
7	d'	Pre-stimulus ERP amplitude	Condition (predictable/ unpredictable) Position (A/B/C/D) LPC amplitude	+ Subject	By-subject according to condition

Figure 5. LPC grand averages

Grand average ERPs at channels C3, P3, Pz, and Cz (for visualisation purposes), with the LPC time window shaded grey, according to condition. Black dotted lines depict the onset of each image in the sequence, and grey dotted lines denote the end of image presentation. Green lines represent N400 data belonging to the predictable condition, whilst pink lines reflect the unpredictable condition. Green and pink shading represents the standard errors for each condition.

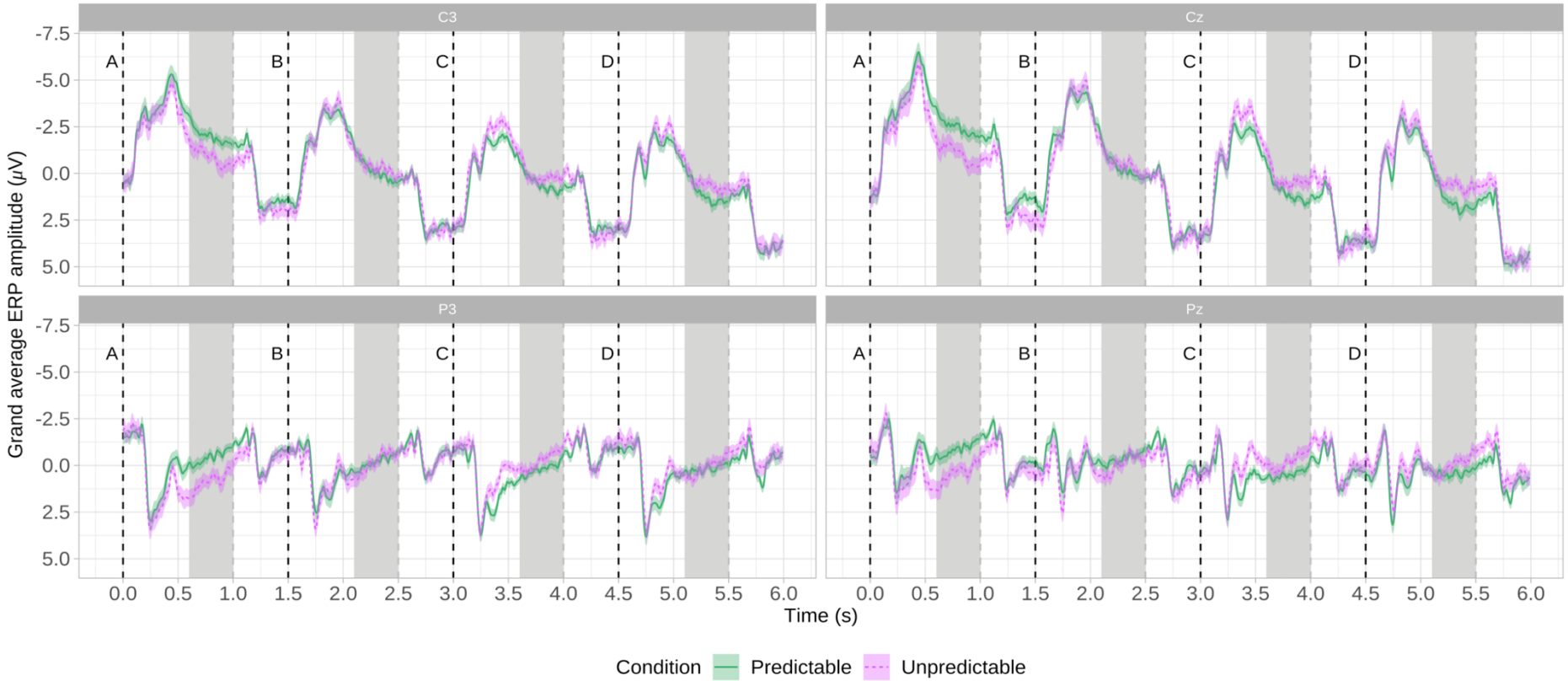

Figure 6. LPC effects
Linear mixed model results depicting the interaction between image condition and position on LPC amplitude. Blue dots represent predictable sequences, whilst pink dots represent unpredictable sequences. Error bars reflect 83% confidence intervals.

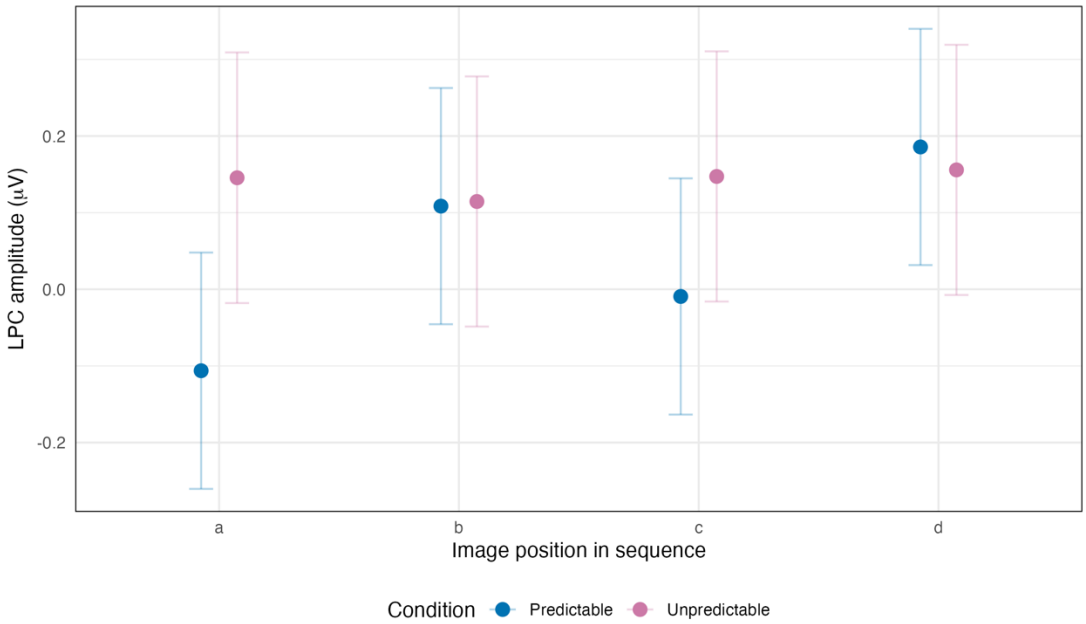

5. Discussion

The present experiment aimed to shed light on the relationship between prediction and memory, by relating N400 activity during exposure to predictable and unpredictable sequences to memory recognition outcomes. Here, we show that whilst memory performance did not differ between predictable and unpredictable conditions *overall* (contrary to our hypothesis), memory was strongest for predictable images in the 'B' sequence position; a finding that will be subsequently discussed in relation to precision and attentional mechanisms. Strikingly, greater N400 amplitudes during learning were associated with better memory outcomes at test for low versus high IAF individuals. This suggests that whilst prediction errors may drive memory encoding, this effect may be modulated according to intrinsic neural differences. Note however, that the 1/f aperiodic slope did not influence this relationship, suggesting that IAF may be particularly relevant for prediction error processing and subsequent memory outcomes. Finally, exploratory analyses revealed a relationship between image condition and position on LPC amplitude. Overall, the current findings contribute novel insight regarding the role of inter-subject differences, attention, and precision in modulating the relationship between prediction and learning.

5.1. Prediction errors may drive memory encoding via increases in precision

Although memory recognition overall did not differ between predictable and unpredictable sequences, memory was best for predictable images in the 'B' position. While at a surface level, this finding may suggest that predictions enhance memory, a closer look at the importance of the 'B' image position for sequence processing may provide stronger support for the role of prediction errors in driving memory encoding. Not only was the 'B' image predictable and predictive of the upcoming 'C' and 'D' items, but it was likely the first image that confirmed whether the sequence was unfolding in a predictable manner. As such, it is

possible that predictable images in this position were attended to more strongly than other images, due to their relevance for evaluating the sequence. In predictive coding, attention is proposed to reflect judgements concerning the *precision* of a stimulus; that is, the amount of certainty or variance in the signal (Bastos et al., 2012; Feldman & Friston, 2010; Friston et al., 2011). Attention increases the synaptic gain of prediction error-encoding neuronal populations, thus affording a stronger precision-weighting to a sensory stimulus and enhancing its ability to prompt model updating (Feldman & Friston, 2010). In the present study, attention may have been directed towards the predictable 'B' images once participants learnt their relevance for the broader sequence, leading to increased precision-weightings. Stronger error signals due to greater precision may have consequently triggered a switch to memory encoding, thus explaining how increases in stimulus precision may have led to enhanced memory.

This explanation is further complemented by the observation that N400 amplitudes were generally greatest for images in the 'B' position, with the N400 proposed to not only reflect a prediction error, but to be indicative of a *precision-weighted* prediction error signal that is dependent on stimulus uncertainty (Bornkessel-Schlesewsky & Schlesewsky, 2019). As such, greater N400 amplitudes may reflect stronger precision-weighted errors, potentially due to enhanced attention toward the 'B' images. Our behavioural results therefore provide insight into how predictions accumulate across sequences, by suggesting that in longer sequences, the brain may prioritise the items deemed most informative, and direct attention away from subsequent items if the prior information is sufficient for predictive processing. This is supported by Darriba & Waszak (2018), who investigated predictions across four-item sequences. Increases in the P2a and P3 ERP components (proposed to reflect evidence accumulation) were observed from the first to the third stimulus, but not at the final stimulus in the predictable sequences (Darriba & Waszak, 2018). Consequently, it was suggested that evidence accumulates until sufficient information for the prediction is acquired, potentially explaining the prioritisation of the 'B' image observed here. However, it is important to note that whilst we assume that the 'B' images received more attention, this was not explicitly measured, and future research may benefit from relating more direct measures of attention (e.g., eye-tracking; Carter & Luke, 2020) to prediction errors during sequence learning.

To explain why images in predictable sequences elicited prediction errors at all, we also highlight a crucial aspect of our study design: whilst predictable sequences promoted predictions about upcoming image categories, item-specific prediction violations for images could still be evoked as each item was unique. This distinction between category and item-based predictions is congruent with hierarchical predictive coding, where predictions at higher levels may code for more integrative relationships (e.g., sequential categorical associations), whilst predictions at lower levels pertain to more basic (e.g., item-specific) attributes (Rao & Ballard, 1999; Rauss & Pourtois, 2013). This may lead to prediction errors that enhance memory at the item-level, which importantly, is also the level at which memory recognition was tested. Therefore, whilst at a superficial level, our behavioural findings suggest that predictable information is better remembered, an interpretation based on precision lends stronger support to the view that prediction errors at the item-level prompted memory encoding via increased attention.

5.2. Prediction errors may enhance memory via reconsolidation processes

Whilst our behavioural results may suggest that stimulus precision leads to stronger memory for prediction error-inducing data, findings relating the N400 to memory performance can more directly clarify assumptions regarding the effect of prediction on memory. Notably, we observed a positive relationship between N400 amplitude and memory performance for

individuals with a low IAF, whilst this effect was absent for those with a high IAF. Based on the N400's link to prediction error (Bornkessel-Schlesewsky & Schlesewsky, 2019; Fitz & Chang, 2019; Hodapp & Rabovsky, 2021; Rabovsky et al., 2018), this finding suggests that for some individuals, greater prediction error signals during learning promoted memory encoding. This is in line with prior research, which proposes that prediction errors drive memory updating via memory reconsolidation mechanisms (Exton-McGuinness et al., 2015; Fernández et al., 2016; Sinclair et al., 2021; Sinclair & Barense, 2019). Reconsolidation is the process by which an existing memory is reactivated, becoming unstable and prone to change, whether that be interference or memory strengthening (Sinclair & Barense, 2019). When a stimulus is encountered, a memory trace for a previously learnt association is reactivated (Kveraga et al., 2007; Sinclair & Barense, 2019). Prediction errors then weaken the associations between the originally learnt items, prompting reconsolidation and enabling the new information to be updated into the existing memory representation (Exton-McGuinness et al., 2015; Sinclair & Barense, 2019). This effect appears contingent on the magnitude of the prediction error, with minimal prediction errors seeming insufficient to prompt reconsolidation and updating of the new, error-inducing information into memory (Gura et al., 2020). In the present study, greater prediction error signals may have prompted memory reconsolidation, where the error-eliciting information was updated into the existing memory trace. As such, our study provides novel evidence for the role of the N400 as a prediction error signal that enhances memory in contexts that extend beyond language. However, the modulation of this effect according to IAF also highlights the importance of individual factors in this relationship.

5.3. The effect of prediction on memory is modulated by individual alpha frequency (IAF)

The present study is the first to our knowledge to demonstrate a role for intrinsic neural activity in modulating the effect of prediction errors on memory, emphasising that whilst prediction may be a fundamental mechanism within the brain (Friston, 2010; Kveraga et al., 2007), it's role in learning is subject to between-participant variation. For individuals with a low IAF, larger N400 amplitudes were associated with better memory. However, this trend was not observed for those with a high IAF, suggesting that the effect of prediction error on memory may differ between individuals. A high IAF has been linked to better general cognitive ability (Grandy et al., 2013) and to faster information processing speeds, reflected by shorter reaction times (Klimesch et al., 1996; Surwillo, 1961, 1963) and more accurate responses to near-threshold stimuli (Samaha & Postle, 2015). Regarding prediction, this rapid information processing may lead to faster perceptual sampling of external stimuli and hence a stronger tendency towards model updating (i.e., memory encoding; Kurthen et al., 2020). This is supported by Cross and colleagues' (2020) study on emotional memory, where high IAF individuals exhibited stronger memory for both neutral and positive stimuli, in contrast to low IAF individuals. Here, negative information was argued to be of greatest importance, and from this it was suggested that high IAF individuals may possess a heightened ability to encode less relevant information into memory (Cross et al., 2020). A key aspect of predictive coding is that whilst the brain must update predictions according to errors, it must also understand which errors are most relevant for learning (Van De Cruys et al., 2014). This rests on precision (also described above), where judgements concerning the certainty of a stimulus act as "meta-predictions" or "second-order predictions" that delegate the extent to which sensory information drives model updating (Kanai et al., 2015; Van De Cruys et al., 2014). In the present study, high IAF individuals may have attributed stronger precision-weightings to sensory data that was less relevant for the future. This may have resulted in the encoding of that information, potentially distorting the predictive model that was applied, and impairing subsequent recognition performance. Further, whilst this effect did not differ according to whether the images were in the predictable or unpredictable sequences, item-based prediction

errors were still likely elicited by both conditions as participants attempted to learn the underlying relationships between the sequences (even in the unpredictable sequences, where unbeknownst to participants, a relationship was absent). Therefore, the current results emphasise the role of individual differences in prediction, by suggesting that *what* is updated into the prediction may be as important for learning as the updating process itself. Alternatively, whilst it is proposed that prediction errors prompt model updating (Friston, 2005), further research would be beneficial to confirm this assumption, as the present findings at face value could also suggest that updating (in a memory encoding sense) may not always occur for some individuals. Ultimately, our results demonstrate that even in simple paradigms, differential prediction and error-processing tendencies may lead to distinct memory outcomes, providing a potential explanation for inter-subject differences in memory performance.

5.4. The relationship between prediction and the late positive complex (LPC)

Whilst the observed N400 effects suggest that prediction errors drive memory reconsolidation for some individuals, differences in the LPC may be explained by its ties to the P300 component. Traditionally, the LPC has been observed during the test phase of memory recognition paradigms, demonstrating greater (i.e., more positive) amplitudes for old versus new items, and is thus proposed to reflect processes relating to episodic recollection (Curran, 2000; Curran & Cleary, 2003). Interestingly, we observed LPC differences at the 'A' and 'C' image positions, such that LPC amplitudes were greater for unpredictable versus predictable images. As each image in the learning phase was unique, items seen during this phase could not be explicitly 'recognised,' rendering it difficult to explain the observed differences in this component from a purely recollection-based account. However, it is possible that effects here reflect recognition at the category level, as compared to specific episodic recollection, such that LPC amplitudes differed according to recollection of the various image categories.

Although LPC effects during learning may reflect category-based recollection, the LPC has also been linked to the P300 ERP component, often being described as a late 'P300' or 'P600' (Finnigan et al., 2002). The P300 component is modulated by stimulus probability and relevance (Berlad & Pratt, 1995; Polich & Margala, 1997), and is commonly observed in oddball paradigms, in response to deviant target stimuli that are presented amongst standard stimuli (Picton, 1992). For this reason, classical conceptions of the component link it to context updating (i.e., a need to revise one's schema of the current context following a contextual change; Donchin, 1981). This notion of 'context updating' may bear similarities to predictive model updating, potentially providing an explanation for the smaller LPC amplitudes to predictable 'A' and 'C' images observed here. If the LPC is a late P300, decreased LPC amplitudes for predictable 'A' and C' images may reflect a diminished need to update a model or context representation. As such images belong to the 'predictable' condition, they are less likely to signal a change in the sequence, and therefore to necessitate contextual or memory updating. Consequently, it would be reasonable to predict that stronger LPC amplitudes would translate to better memory performance. However, LPC amplitudes were not related to memory outcomes in the present experiment. Here, it is possible that memory for the broader categorical relationship was updated, as opposed to memory for specific items. However, further research would be necessary to consolidate this theory with hierarchical predictive coding notions (Rao & Ballard, 1999), where theoretically, the updating of higher-level models should not bypass lower-level (e.g., item-specific) representations. Nevertheless, the present results suggest that changes in the LPC component are susceptible to item predictability and sequential position.

5.5. Conclusion

Our results strongly suggest that prediction errors (as measured via the N400) drive memory encoding, potentially via reconsolidation-based mechanisms (Exton-McGuinness et al., 2015; Fernández et al., 2016; Sinclair & Barense, 2019). The findings also shed light on predictive processing across longer sequences of information, by suggesting that attention may be directed towards stimuli deemed most informative, thus increasing stimulus precision and the extent to which prediction errors prompt model updating (Feldman & Friston, 2010). Notably, we show that individual neural factors modulate the relationship between prediction errors and memory, suggesting that whilst prediction could underlie cognition more generally (Friston, 2010; Kveraga et al., 2007), prediction tendencies may differ between individuals to affect information uptake. Therefore, this study offers novel insights into prediction and memory, by highlighting the importance of individual factors for building a complete picture of memory processing.

Declaration of Generative AI and AI-assisted technologies in the writing process

During the preparation of this work the authors used Chat-GPT sparingly to assist with the refinement of sentences supplied by the authors. After using this tool/service, the authors reviewed and edited the content as needed and take full responsibility for the content of the publication.

Reference list

Alday, P. M. (2019). How much baseline correction do we need in ERP research? Extended GLM model can replace baseline correction while lifting its limits. *Psychophysiology*, *56*(12), e13451. https://doi.org/10.1111/psyp.13451

Appelhoff, S., Sanderson, M., Brooks, T. L., Vliet, M. van, Quentin, R., Holdgraf, C., Chaumon, M., Mikulan, E., Tavabi, K., Höchenberger, R., Welke, D., Brunner, C., Rockhill, A. P., Larson, E., Gramfort, A., & Jas, M. (2019). MNE-BIDS: Organizing electrophysiological data into the BIDS format and facilitating their analysis. *Journal of Open Source Software*, *4*(44), 1896. https://doi.org/10.21105/joss.01896

Baker, R., Dexter, M., Hardwicke, T. E., Goldstone, A., & Kourtzi, Z. (2014). Learning to predict: Exposure to temporal sequences facilitates prediction of future events. *Vision Research*, *99*, 124–133. https://doi.org/10.1016/j.visres.2013.10.017

Bar, M. (2007). The proactive brain: Using analogies and associations to generate predictions. *Trends in Cognitive Sciences*, *11*(7), 280–289. https://doi.org/10.1016/j.tics.2007.05.005

Barron, H. C., Auksztulewicz, R., & Friston, K. (2020). Prediction and memory: A predictive coding account. *Progress in Neurobiology*, *192*, 101821. https://doi.org/10.1016/j.pneurobio.2020.101821

Bastos, A. M., Usrey, W. M., Adams, R. A., Mangun, G. R., Fries, P., & Friston, K. J. (2012). Canonical Microcircuits for Predictive Coding. *Neuron*, *76*(4), 695–711. https://doi.org/10.1016/j.neuron.2012.10.038

Bates, D., Kliegl, R., Vasishth, S., & Baayen, H. (2018). Parsimonious Mixed Models. *arXiv:1506.04967 [Stat]*. http://arxiv.org/abs/1506.04967

Bates, D., Mächler, M., Bolker, B., & Walker, S. (2014). Fitting Linear Mixed-Effects Models using lme4. *arXiv:1406.5823 [Stat]*. http://arxiv.org/abs/1406.5823

Bein, O., Gasser, C., Amer, T., Maril, A., & Davachi, L. (2023). Predictions transform memories: How expected versus unexpected events are integrated or separated in memory. *Neuroscience & Biobehavioral Reviews*, 105368. https://doi.org/10.1016/j.neubiorev.2023.105368

Berlad, I., & Pratt, H. (1995). P300 in response to the subject's own name. *Electroencephalography and Clinical Neurophysiology/Evoked Potentials Section*, *96*(5), 472–474. https://doi.org/10.1016/0168-5597(95)00116-A

Besson, M., Kutas, M., & Petten, C. V. (1992). An Event-Related Potential (ERP) Analysis of Semantic Congruity and Repetition Effects in Sentences. *Journal of Cognitive Neuroscience*, *4*(2), 132–149. https://doi.org/10.1162/jocn.1992.4.2.132

Bornkessel-Schlesewsky, I., Sharrad, I., Howlett, C. A., Alday, P. M., Corcoran, A. W., Bellan, V., Wilkinson, E., Kliegl, R., Lewis, R. L., Small, S. L., & Schlesewsky, M. (2022). Rapid adaptation of predictive models during language comprehension: Aperiodic EEG slope, individual alpha frequency and idea density modulate individual differences in real-time model updating. *Frontiers in Psychology*, *13*, 1–28. https://doi.org/10.3389/fpsyg.2022.817516

Bornkessel-Schlesewsky, I., & Schlesewsky, M. (2019). Toward a neurobiologically plausible model of language-related, negative event-related potentials. *Frontiers in Psychology*, *10*(298), 1–17. https://doi.org/10.3389/fpsyg.2019.00298

Brezis, N., Bronfman, Z. Z., Yovel, G., & Goshen-Gottstein, Y. (2017). The Electrophysiological Signature of Remember–Know Is Confounded with Memory Strength and Cannot Be Interpreted as Evidence for Dual-process Theory of Recognition. *Journal of Cognitive Neuroscience*, *29*(2), 322–336. https://doi.org/10.1162/jocn_a_01053

Carter, B. T., & Luke, S. G. (2020). Best practices in eye tracking research. *International Journal of Psychophysiology*, *155*, 49–62. https://doi.org/10.1016/j.ijpsycho.2020.05.010

Chow, W.-Y., Momma, S., Smith, C., Lau, E., & Phillips, C. (2016). Prediction as memory retrieval: Timing and mechanisms. *Language, Cognition and Neuroscience*, *31*(5), 617–627. https://doi.org/10.1080/23273798.2016.1160135

Corcoran, A. W., Alday, P. M., Schlesewsky, M., & Bornkessel-Schlesewsky, I. (2018). Toward a reliable, automated method of individual alpha frequency (IAF) quantification. *Psychophysiology*, *55*(7), e13064. https://doi.org/10.1111/psyp.13064

Cross, Z. R., Santamaria, A., Corcoran, A. W., Chatburn, A., Alday, P. M., Coussens, S., & Kohler, M. J. (2020). Individual alpha frequency modulates sleep-related emotional memory consolidation. *Neuropsychologia*, *148*, 107660. https://doi.org/10.1016/j.neuropsychologia.2020.107660

Curran, T. (2000). Brain potentials of recollection and familiarity. *Memory & Cognition*, *28*(6), 923–938. https://doi.org/10.3758/BF03209340

Curran, T., & Cleary, A. M. (2003). Using ERPs to dissociate recollection from familiarity in picture recognition. *Cognitive Brain Research*, *15*(2), 191–205. https://doi.org/10.1016/S0926-6410(02)00192-1

Darriba, Á., & Waszak, F. (2018). Predictions through evidence accumulation over time. *Scientific Reports*, *8*(1), 494. https://doi.org/10.1038/s41598-017-18802-z

[dataset]. Jano, S. Memory, prediction, and individual differences. *Open Science Framework (OSF).* 2023. DOI 10.17605/OSF.IO/QVJER.

Dave, S., Brothers, T. A., & Swaab, T. Y. (2018). 1/f neural noise and electrophysiological indices of contextual prediction in aging. *Brain Research*, *1691*, 34–43. https://doi.org/10.1016/j.brainres.2018.04.007

DeLong, K. A., Urbach, T. P., & Kutas, M. (2005). Probabilistic word pre-activation during language comprehension inferred from electrical brain activity. *Nature Neuroscience*, *8*(8), Article 8. https://doi.org/10.1038/nn1504

Dodd, M. D., & Flowers, J. H. (Eds.). (2012). *The Influence of Attention, Learning, and Motivation on Visual Search*. Springer New York. https://doi.org/10.1007/978-1-4614-4794-8

Donchin, E. (1981). Surprise!… Surprise? *Psychophysiology*, *18*(5), 493–513. https://doi.org/10.1111/j.1469-8986.1981.tb01815.x

Donoghue T, Haller M, Peterson EJ, Varma P, Sebastian P, Gao R, Noto T, Lara AH, Wallis JD, Knight RT, Shestyuk A, Voytek B (2020). *Parameterizing neural power spectra into periodic and aperiodic components. Nature Neuroscience, 23, 1655-1665. DOI: 10.1038/s41593-020-00744-x*.

Exton-McGuinness, M. T. J., Lee, J. L. C., & Reichelt, A. C. (2015). Updating memories—The role of prediction errors in memory reconsolidation. *Behavioural Brain Research*, *278*, 375–384. https://doi.org/10.1016/j.bbr.2014.10.011

Federmeier, K. D., & Kutas, M. (1999). A Rose by Any Other Name: Long-Term Memory Structure and Sentence Processing. *Journal of Memory and Language*, *41*(4), 469–495. https://doi.org/10.1006/jmla.1999.2660

Feldman, H., & Friston, K. J. (2010). Attention, Uncertainty, and Free-Energy. *Frontiers in Human Neuroscience*, *4*. https://doi.org/10.3389/fnhum.2010.00215

Fernández, R. S., Boccia, M. M., & Pedreira, M. E. (2016). The fate of memory: Reconsolidation and the case of Prediction Error. *Neuroscience & Biobehavioral Reviews*, *68*, 423–441. https://doi.org/10.1016/j.neubiorev.2016.06.004

Finnigan, S., Humphreys, M. S., Dennis, S., & Geffen, G. (2002). ERP 'old/new' effects: Memory strength and decisional factor(s). *Neuropsychologia*, *40*(13), 2288–2304. https://doi.org/10.1016/S0028-3932(02)00113-6

Fiser, J., & Aslin, R. N. (2002). Statistical learning of higher-order temporal structure from visual shape sequences. *Journal of Experimental Psychology: Learning, Memory, and Cognition*, *28*, 458–467. https://doi.org/10.1037/0278-7393.28.3.458

Fitz, H., & Chang, F. (2019). Language ERPs reflect learning through prediction error propagation. *Cognitive Psychology*, *111*, 15–52. https://doi.org/10.1016/j.cogpsych.2019.03.002

Fox, J., & Weisberg, S. (2019). *An R Companion to Applied Regression*. SAGE Publications.

Friston, K. (2005). A theory of cortical responses. *Philosophical Transactions of the Royal Society B: Biological Sciences*, *360*(1456), 815–836. https://doi.org/10.1098/rstb.2005.1622

Friston, K. (2009). The free-energy principle: A rough guide to the brain? *Trends in Cognitive Sciences*, *13*(7), 293–301. https://doi.org/10.1016/j.tics.2009.04.005

Friston, K. (2010). The free-energy principle: A unified brain theory? *Nature Reviews Neuroscience*, *11*(2), Article 2. https://doi.org/10.1038/nrn2787

Friston, K., & Kiebel, S. (2009). Predictive Coding under the Free-Energy Principle. *Philosophical Transactions: Biological Sciences*, *364*(1521), 1211–1221.

Friston, K., Mattout, J., & Kilner, J. (2011). Action understanding and active inference. *Biological Cybernetics*, *104*(1), 137–160. https://doi.org/10.1007/s00422-011-0424-z

Furutachi, S., Franklin, A. D., Mrsic-Flogel, T. D., & Hofer, S. B. (2023). *Cooperative thalamocortical circuit mechanism for sensory prediction errors* (p. 2023.07.12.548664). bioRxiv. https://doi.org/10.1101/2023.07.12.548664

Garrido, M. I., Kilner, J. M., Kiebel, S. J., Stephan, K. E., Baldeweg, T., & Friston, K. J. (2009). Repetition suppression and plasticity in the human brain. *NeuroImage*, *48*(1), 269–279. https://doi.org/10.1016/j.neuroimage.2009.06.034

Gavornik, J. P., & Bear, M. F. (2014). Learned spatiotemporal sequence recognition and prediction in primary visual cortex. *Nature Neuroscience*, *17*(5), 732–737. https://doi.org/10.1038/nn.3683

Gramfort, A., Luessi, M., Larson, E., Engemann, D. A., Strohmeier, D., Brodbeck, C., Goj, R., Jas, M., Brooks, T., Parkkonen, L., & Hämäläinen, M. (2013). MEG and EEG data analysis with MNE-Python. *Frontiers in Neuroscience*, *7*(7), 267–267. https://doi.org/10.3389/fnins.2013.00267

Grandy, T. H., Werkle-Bergner, M., Chicherio, C., Lövdén, M., Schmiedek, F., & Lindenberger, U. (2013). Individual alpha peak frequency is related to latent factors of general cognitive abilities. *NeuroImage*, *79*, 10–18. https://doi.org/10.1016/j.neuroimage.2013.04.059

Greve, A., Cooper, E., Kaula, A., Anderson, M. C., & Henson, R. (2017). Does prediction error drive one-shot declarative learning? *Journal of Memory and Language*, *94*, 149–165. https://doi.org/10.1016/j.jml.2016.11.001

Gura, H., Davidson, A., & Gotthard, G. H. (2020). Prediction error parameters for visuospatial interference: Minimal prediction errors leave positive declarative memory intact following visuospatial word search interference. *Learning and Motivation*, *72*, 101674. https://doi.org/10.1016/j.lmot.2020.101674

Habib, R., McIntosh, A. R., Wheeler, M. A., & Tulving, E. (2003). Memory encoding and hippocampally-based novelty/familiarity discrimination networks. *Neuropsychologia*, *41*(3), 271–279. https://doi.org/10.1016/S0028-3932(02)00160-4

Haeuser, K. I., & Kray, J. (2022). How odd: Diverging effects of predictability and plausibility violations on sentence reading and word memory. *Applied Psycholinguistics*, *43*(5), 1193–1220. https://doi.org/10.1017/S0142716422000364

Hautus, M. J. (1995). Corrections for extreme proportions and their biasing effects on estimated values of d′. *Behavior Research Methods, Instruments, & Computers*, *27*(1), 46–51. https://doi.org/10.3758/BF03203619

Hodapp, A., & Rabovsky, M. (2021). The N400 ERP component reflects an error-based implicit learning signal during language comprehension. *European Journal of Neuroscience*, *54*(9), 7125–7140. https://doi.org/10.1111/ejn.15462

Hohwy, J. (2013). *The Predictive Mind*. OUP Oxford.

Jang, A. I., Nassar, M. R., Dillon, D. G., & Frank, M. J. (2019). Positive reward prediction errors during decision-making strengthen memory encoding. *Nature Human Behaviour*, *3*(7), 719–732. https://doi.org/10.1038/s41562-019-0597-3

Jano, S., Cross, Z., Chatburn, A., Schlesewsky, M., & Bornkessel-Schlesewsky, I. (2023). *Predictions in language adapt across contexts and individuals* (p. 2023.05.08.539915). bioRxiv. https://doi.org/10.1101/2023.05.08.539915

Jas, M., Engemann, D., Raimondo, F., Bekhti, yousra, & Gramfort, A. (2016, June). Automated rejection and repair of bad trials in MEG/EEG. *6th International Workshop on Pattern Recognition in Neuroimaging (PRNI)*. https://hal.archives-ouvertes.fr/hal-01313458

Kanai, R., Komura, Y., Shipp, S., & Friston, K. (2015). Cerebral hierarchies: Predictive processing, precision and the pulvinar. *Philosophical Transactions of the Royal Society B: Biological Sciences*, *370*(1668), 20140169. https://doi.org/10.1098/rstb.2014.0169

Kim, H. (2011). Neural activity that predicts subsequent memory and forgetting: A meta-analysis of 74 fMRI studies. *NeuroImage*, *54*(3), 2446–2461. https://doi.org/10.1016/j.neuroimage.2010.09.045

Kim, H., Schlichting, M. L., Preston, A. R., & Lewis-Peacock, J. A. (2020). Predictability Changes What We Remember in Familiar Temporal Contexts. *Journal of Cognitive Neuroscience*, *32*(1), 124–140. https://doi.org/10.1162/jocn_a_01473

Klimesch, W., Doppelmayr, M., Schimke, H., & Pachinger, T. (1996). Alpha Frequency, Reaction Time, and the Speed of Processing Information. *Journal of Clinical Neurophysiology*, *13*(6), 511–518.

Kurthen, I., Meyer, M., Schlesewsky, M., & Bornkessel-Schlesewsky, I. (2020). Individual Differences in Peripheral Hearing and Cognition Reveal Sentence Processing Differences in Healthy Older Adults. *Frontiers in Neuroscience*, *14*. https://doi.org/10.3389/fnins.2020.573513

Kutas, M., & Federmeier, K. D. (2011). Thirty Years and Counting: Finding Meaning in the N400 Component of the Event-Related Brain Potential (ERP). *Annual Review of Psychology*, *62*(1), 621–647. https://doi.org/10.1146/annurev.psych.093008.131123

Kutas, M., & Hillyard, S. A. (1980). Reading Senseless Sentences: Brain Potentials Reflect Semantic Incongruity. *Science*, *207*(4427), 203–205.

Kutas, M., & Hillyard, S. A. (1984). Brain potentials during reading reflect word expectancy and semantic association. *Nature*, *307*(5947), Article 5947. https://doi.org/10.1038/307161a0

Kveraga, K., Ghuman, A. S., & Bar, M. (2007). Top-down predictions in the cognitive brain. *Brain and Cognition*, *65*(2), 145–168. https://doi.org/10.1016/j.bandc.2007.06.007

Long, N. M., Lee, H., & Kuhl, B. A. (2016). Hippocampal Mismatch Signals Are Modulated by the Strength of Neural Predictions and Their Similarity to Outcomes. *The Journal*

of Neuroscience, *36*(50), 12677–12687. https://doi.org/10.1523/JNEUROSCI.1850-16.2016

Mack, M. L., Love, B. C., & Preston, A. R. (2018). Building concepts one episode at a time: The hippocampus and concept formation. *Neuroscience Letters*, *680*, 31–38. https://doi.org/10.1016/j.neulet.2017.07.061

Makowski, D. (2018). The psycho Package: An Efficient and Publishing-Oriented Workflow for Psychological Science. *Journal of Open Source Software*, *3*(22), 470. https://doi.org/10.21105/joss.00470

Mathôt, S., Schreij, D., & Theeuwes, J. (2012). OpenSesame: An open-source, graphical experiment builder for the social sciences. *Behavior Research Methods*, *44*(2), 314–324. https://doi.org/10.3758/s13428-011-0168-7

McNicol, D. (2005). *A Primer of Signal Detection Theory*. Psychology Press.

Meyer, P., Mecklinger, A., & Friederici, A. D. (2007). Bridging the gap between the semantic N400 and the early old/new memory effect. *NeuroReport*, *18*(10), 1009. https://doi.org/10.1097/WNR.0b013e32815277eb

Michelon, P., Snyder, A. Z., Buckner, R. L., McAvoy, M., & Zacks, J. M. (2003). Neural correlates of incongruous visual information: an event-related fMRI study. *NeuroImage*, *19*(4), 1612–1626. https://doi.org/10.1016/S1053-8119(03)00111-3

Otsuka, S., & Saiki, J. (2016). Gift from statistical learning: Visual statistical learning enhances memory for sequence elements and impairs memory for items that disrupt regularities. *Cognition*, *147*, 113–126. https://doi.org/10.1016/j.cognition.2015.11.004

Parr, T., Pezzulo, G., & Friston, K. J. (2022). *Active Inference: The Free Energy Principle in Mind, Brain, and Behavior*. https://doi.org/10.7551/mitpress/12441.001.0001

Picton, T. (1992). The P300 Wave of the Human Event-Related Potential. *Journal of Clinical Neurophysiology : Official Publication of the American Electroencephalographic Society*, *9*, 456–479. https://doi.org/10.1097/00004691-199210000-00002

Polich, J., & Margala, C. (1997). P300 and probability: Comparison of oddball and single-stimulus paradigms. *International Journal of Psychophysiology*, *25*(2), 169–176. https://doi.org/10.1016/S0167-8760(96)00742-8

Quent, J. A., Greve, A., & Henson, R. N. (2022). Shape of U: The Nonmonotonic Relationship Between Object–Location Memory and Expectedness. *Psychological Science*, *33*(12), 2084–2097. https://doi.org/10.1177/09567976221109134

Rabovsky, M., Hansen, S. S., & McClelland, J. L. (2018). Modelling the N400 brain potential as change in a probabilistic representation of meaning. *Nature Human Behaviour*, *2*(9), Article 9. https://doi.org/10.1038/s41562-018-0406-4

Rao, R. P. N., & Ballard, D. H. (1999). Predictive coding in the visual cortex: A functional interpretation of some extra-classical receptive-field effects. *Nature Neuroscience*, *2*(1), Article 1. https://doi.org/10.1038/4580

Rauss, K., & Born, J. (2017). A Role of Sleep in Forming Predictive Codes. In N. Axmacher & B. Rasch (Eds.), *Cognitive Neuroscience of Memory Consolidation* (pp. 117–132). Springer International Publishing. https://doi.org/10.1007/978-3-319-45066-7_8

Rauss, K., & Pourtois, G. (2013). What is Bottom-Up and What is Top-Down in Predictive Coding? *Frontiers in Psychology*, *4*. https://www.frontiersin.org/article/10.3389/fpsyg.2013.00276

Rouhani, N., Norman, K. A., & Niv, Y. (2018). Dissociable effects of surprising rewards on learning and memory. *Journal of Experimental Psychology: Learning, Memory, and Cognition*, *44*(9), 1430–1443. https://doi.org/10.1037/xlm0000518

Rouhani, N., Norman, K. A., Niv, Y., & Bornstein, A. M. (2020). Reward prediction errors create event boundaries in memory. *Cognition*, *203*, 104269–104269. https://doi.org/10.1016/j.cognition.2020.104269

Saffran, J. R., Newport, E. L., & Aslin, R. N. (1996). Word Segmentation: The Role of Distributional Cues. *Journal of Memory and Language*, *35*(4), 606–621. https://doi.org/10.1006/jmla.1996.0032

Samaha, J., & Postle, B. R. (2015). The Speed of Alpha-Band Oscillations Predicts the Temporal Resolution of Visual Perception. *Current Biology*, *25*(22), 2985–2990. https://doi.org/10.1016/j.cub.2015.10.007

Schoknecht, P., Roehm, D., Schlesewsky, M., & Bornkessel-Schlesewsky, I. (2022). The interaction of predictive processing and similarity-based retrieval interference: An ERP study. *Language, Cognition and Neuroscience*, *0*(0), 1–19. https://doi.org/10.1080/23273798.2022.2026421

Schwarb, H., & Schumacher, E. H. (2012). Generalized lessons about sequence learning from the study of the serial reaction time task. *Advances in Cognitive Psychology*, *8*(2), 165–178. https://doi.org/10.2478/v10053-008-0113-1

Sherman, B. E., Graves, K. N., Huberdeau, D. M., Quraishi, I. H., Damisah, E. C., & Turk-Browne, N. B. (2022). Temporal Dynamics of Competition between Statistical Learning and Episodic Memory in Intracranial Recordings of Human Visual Cortex. *Journal of Neuroscience*, *42*(48), 9053–9068. https://doi.org/10.1523/JNEUROSCI.0708-22.2022

Sherman, B. E., & Turk-Browne, N. B. (2020). Statistical prediction of the future impairs episodic encoding of the present. *Proceedings of the National Academy of Sciences*, *117*(37), 22760–22770. https://doi.org/10.1073/pnas.2013291117

Siegelman, N., Bogaerts, L., & Frost, R. (2017). Measuring individual differences in statistical learning: Current pitfalls and possible solutions. *Behavior Research Methods*, *49*(2), 418–432. https://doi.org/10.3758/s13428-016-0719-z

Siegelman, N., & Frost, R. (2015). Statistical learning as an individual ability: Theoretical perspectives and empirical evidence. *Journal of Memory and Language*, *81*, 105–120. https://doi.org/10.1016/j.jml.2015.02.001

Sinclair, A. H., & Barense, M. D. (2019). Prediction Error and Memory Reactivation: How Incomplete Reminders Drive Reconsolidation. *Trends in Neurosciences*, *42*(10), 727–739. https://doi.org/10.1016/j.tins.2019.08.007

Sinclair, A. H., Manalili, G. M., Brunec, I. K., Adcock, R. A., & Barense, M. D. (2021). Prediction errors disrupt hippocampal representations and update episodic memories. *Proceedings of the National Academy of Sciences*, *118*(51), e2117625118. https://doi.org/10.1073/pnas.2117625118

Stróżak, P., Bird, C. W., Corby, K., Frishkoff, G., & Curran, T. (2016). FN400 and LPC memory effects for concrete and abstract words. *Psychophysiology*, *53*(11), 1669–1678. https://doi.org/10.1111/psyp.12730

Surwillo, W. W. (1961). Frequency of the 'Alpha' Rhythm, Reaction Time and Age. *Nature*, *191*(4790), Article 4790. https://doi.org/10.1038/191823a0

Surwillo, W. W. (1963). The relation of simple response time to brain-wave frequency and the effects of age. *Electroencephalography and Clinical Neurophysiology*, *15*(1), 105–114. https://doi.org/10.1016/0013-4694(63)90043-9

Turan, G., Ehrlich, I., Shing, Y. L., & Nolden, S. (2023). *From generating to violating predictions: The effects of prediction error on episodic memory*. PsyArXiv. https://doi.org/10.31234/osf.io/zm29a

Urgen, B. A., Kutas, M., & Saygin, A. P. (2018). Uncanny valley as a window into predictive processing in the social brain. *Neuropsychologia*, *114*, 181–185. https://doi.org/10.1016/j.neuropsychologia.2018.04.027

Van De Cruys, S., Evers, K., Van Der Hallen, R., Van Eylen, L., Boets, B., de-Wit, L., & Wagemans, J. (2014). Precise minds in uncertain worlds: Predictive coding in autism. *Psychological Review*, *121*(4), 649–675. https://doi.org/10.1037/a0037665

Van Kesteren, M. T. R., Ruiter, D. J., Fernández, G., & Henson, R. N. (2012). How schema and novelty augment memory formation. *Trends in Neurosciences*, *35*(4), 211–219. https://doi.org/10.1016/j.tins.2012.02.001

Wickham, H. (2016). *Ggplot2 citation info*. Retrieved March 25, 2021, from https://cran.r-project.org/web/packages/ggplot2/citation.html

Worthen, J. B., & Roark, B. (2002). Free Recall Accuracy for Common and Bizarre Verbal Information. *The American Journal of Psychology*, *115*(3), 377–394. https://doi.org/10.2307/1423423

Yang, H., Laforge, G., Stojanoski, B., Nichols, E. S., McRae, K., & Köhler, S. (2019). Late positive complex in event-related potentials tracks memory signals when they are decision relevant. *Scientific Reports*, *9*(1), Article 1. https://doi.org/10.1038/s41598-019-45880-y

6. Appendix 1 – Statistical model outputs

*6.1. Model 1: dprime ~ condition * cog_scale + condition * slope_scale + (1|subjnr), data= behav_indiv*

```
Analysis of Deviance Table (Type II Wald chisquare tests)

Response: dprime
                      Chisq Df Pr(>Chisq)
condition            1.9766  1     0.1598
cog_scale            2.1886  1     0.1390
slope_scale          0.0878  1     0.7670
condition:cog_scale  0.6780  1     0.4103
condition:slope_scale 1.3166  1     0.2512
---
Signif. codes:  0 ***, 0.001**, 0.01*, 0.05.


# Indices of model performance

AIC     |    AICc |     BIC | R2 (cond.) | R2 (marg.) |   ICC |  RMSE |
Sigma
------------------------------------------------------------------------
------
307.592 | 308.244 | 335.097 |      0.044 |      0.029 | 0.016 | 0.421 |
0.430
```

*6.2. Model 2: dprime ~ imagetype * cog_scale + imagetype * slope_scale + (1|subjnr), data= behav_indiv*

```
Analysis of Deviance Table (Type II Wald chisquare tests)

Response: dprime
                       Chisq Df Pr(>Chisq)
imagetype             50.9653  4   2.27e-10 ***
cog_scale              2.1886  1     0.1390
slope_scale            0.0878  1     0.7670
imagetype:cog_scale    3.7278  4     0.4441
imagetype:slope_scale  4.1881  4     0.3811
---
Signif. codes:  0 ***, 0.001**, 0.01*, 0.05.


# Indices of model performance

AIC     |    AICc |     BIC | R2 (cond.) | R2 (marg.) |   ICC |  RMSE |
Sigma
-----------------------------------------------------------------------
------
313.484 | 316.371 | 371.931 |      0.250 |      0.199 | 0.063 | 0.364 |
0.386
```

*6.3. Model 3: N4mean ~ condition * position + prestim_amp_scale + (1+condition|subjnr) + (1|item_no), data= N4_sum1*

```
Analysis of Deviance Table (Type II Wald chisquare tests)

Response: N400amp_mean
                      Chisq Df Pr(>Chisq)
condition            1.2403  1    0.26542
position            41.0797  3   6.29e-09 ***
prestim_amp_scale 9256.2519  1  < 2.2e-16 ***
condition:position   8.0896  3    0.04419 *
---
Signif. codes:  0 ***, 0.001**, 0.01*, 0.05.


# Indices of model performance

AIC       |      AICc |       BIC | R2 (cond.) | R2 (marg.) |   ICC |
RMSE | Sigma
-----------------------------------------------------------------------
------------
3.174e+05 | 3.174e+05 | 3.175e+05 |      0.205 |      0.145 | 0.071 |
4.726 | 4.732
```

*6.4. Model 4: dprime~ condition * position * N400amp_scale * cog_scale + prestim_amp_scale + (1+condition|subjnr), data= N4_sum*

```
Analysis of Deviance Table (Type II Wald chisquare tests)

Response: dprime
                                          Chisq Df Pr(>Chisq)
condition                                4.5271  1   0.033361 *
position                                36.5846  3  5.633e-08 ***
N400amp_scale                            5.9736  1   0.014522 *
cog_scale                                5.5366  1   0.018622 *
prestim_amp_scale                        1.4208  1   0.233264
condition:position                      41.0432  3  6.403e-09 ***
condition:N400amp_scale                  0.0159  1   0.899565
position:N400amp_scale                   1.9143  3   0.590392
condition:cog_scale                      0.2071  1   0.649035
position:cog_scale                       2.8871  3   0.409360
N400amp_scale:cog_scale                  7.5882  1   0.005875 **
condition:position:N400amp_scale         1.6228  3   0.654224
condition:position:cog_scale             2.6895  3   0.442015
condition:N400amp_scale:cog_scale        2.5164  1   0.112671
position:N400amp_scale:cog_scale         0.2516  3   0.968850
condition:position:N400amp_scale:cog_scale  0.2615  3   0.967096
---
Signif. codes:  0 ***, 0.001**, 0.01*, 0.05.


# Indices of model performance

AIC     |    AICc |     BIC | R2 (cond.) | R2 (marg.) |   ICC |  RMSE |
Sigma
-----------------------------------------------------------------------
------
459.242 | 467.763 | 603.841 |      0.466 |      0.198 | 0.334 | 0.263 |
0.297
```

*6.5. Model 5: dprime~ condition * position * N400amp_scale * slope_scale + prestim_amp_scale + (1+condition|subjnr), data= N4_sum*

```
Analysis of Deviance Table (Type II Wald chisquare tests)

Response: dprime
                                            Chisq Df Pr(>Chisq)
condition                                  5.1646  1    0.02305 *
position                                  38.5385  3  2.174e-08 ***
N400amp_scale                              5.0417  1    0.02474 *
slope_scale                                1.3963  1    0.23734
prestim_amp_scale                          1.5373  1    0.21501
condition:position                        43.7228  3  1.728e-09 ***
condition:N400amp_scale                    0.2257  1    0.63477
position:N400amp_scale                     1.7015  3    0.63661
condition:slope_scale                      2.2678  1    0.13209
position:slope_scale                       0.9144  3    0.82195
N400amp_scale:slope_scale                  0.1615  1    0.68776
condition:position:N400amp_scale           1.2515  3    0.74067
condition:position:slope_scale             1.2471  3    0.74174
condition:N400amp_scale:slope_scale        0.0172  1    0.89564
position:N400amp_scale:slope_scale         1.1464  3    0.76587
condition:position:N400amp_scale:slope_scale  1.3827  3    0.70960
---
Signif. codes:  0 ***, 0.001**, 0.01*, 0.05.


# Indices of model performance

AIC     |    AICc |     BIC | R2 (cond.) | R2 (marg.) |   ICC |  RMSE |
Sigma
-----------------------------------------------------------------------
------
478.487 | 486.614 | 624.661 |      0.473 |      0.178 | 0.358 | 0.258 |
0.294
```

*6.6. Model 6: LPCmean ~ condition * position + prestim_amp_scale + (1|subjnr) + (1|item_no), data= LPC_sum1*

```
Analysis of Deviance Table (Type II Wald chisquare tests)

Response: LPCamp_mean
                       Chisq Df Pr(>Chisq)
condition              2.9587  1    0.08542 .
position              47.1361  3  3.252e-10 ***
prestim_amp_scale  66862.1819  1  < 2.2e-16 ***
condition:position    24.6274  3  1.847e-05 ***
---
Signif. codes:  0 ***, 0.001**, 0.01*, 0.05.


# Indices of model performance

AIC       |      AICc |       BIC | R2 (cond.) | R2 (marg.) |   ICC |
RMSE | Sigma
-----------------------------------------------------------------------
------------
5.711e+05 | 5.711e+05 | 5.712e+05 |      0.413 |      0.385 | 0.045 |
3.515 | 3.517
```

*6.7. Model 7: dprime~ condition * position * LPCamp_scale + prestim_amp_scale + (1+condition|subjnr), data= LPC_sum*

```
Analysis of Deviance Table (Type II Wald chisquare tests)

Response: dprime
                                 Chisq Df Pr(>Chisq)
condition                       5.2890  1    0.02146 *
position                       45.1769  3  8.485e-10 ***
LPCamp_scale                    0.0159  1    0.89971
prestim_amp_scale               0.7529  1    0.38555
condition:position             44.4668  3  1.201e-09 ***
condition:LPCamp_scale          2.4649  1    0.11642
position:LPCamp_scale           3.7990  3    0.28401
condition:position:LPCamp_scale 3.7725  3    0.28710
---
Signif. codes:  0 ***, 0.001**, 0.01*, 0.05.


# Indices of model performance

AIC     |    AICc |     BIC | R2 (cond.) | R2 (marg.) |   ICC |  RMSE |
Sigma
-----------------------------------------------------------------------
------
362.195 | 364.747 | 445.158 |      0.482 |      0.157 | 0.385 | 0.258 |
0.288
```